Hot-Spot Dynamics: Quenching, Ignition, Flame Propagation and Extinction

Jeffrey Santner, S. Scott Goldsborough
Argonne National Laboratory
Argonne, IL, USA

1 Abstract

In the elevated pressure and temperature environment in rapid compression machines (RCMs) and engines, flame kernel formation and growth is a complex process. In fundamental RCM experiments, this is thought to affect mild ignition, thus complicating modeling efforts. In engines, this process can cause pre-ignition heat release, altering combustion timing, reducing efficiency, and in some cases leading to knock. Flame kernels in these geometries can form due to heterogeneous temperature and mixture fields. The present work parametrically investigates flame kernel formation and extinction behavior over a range of temperature inhomogeneities that might be present within an RCM. We find that flame formation is primarily governed by competition between hot-spot dissipation and ignition, while flame extinction is governed by flame structure and Lewis number (Le) effects.

2 Introduction

In fundamental kinetic studies performed in rapid compression machines (RCM) and shock tubes, mild ignition complicates modeling efforts and can limit conditions that can be investigated. Mild ignition is observed when a deflagration wave is initiated within the reaction chamber. This flame can consume the mixture, or contribute to early volumetric ignition through compression heating of the unburned mixture. These flames have been identified in RCMs using Schlieren imaging, chemiluminescence, particle image velocimetry, and planar laser induced fluorescence [1–5]. Similarly, pre-ignition heat release in engines can be caused by unwanted flame propagation in the unburned mixture. Both of these issues may be caused in part by flame kernel formation due to temperature inhomogeneities. Damaging engine knock [6] caused by transition to detonation, is outside the scope of this work. We focus on low hot-spot energies and mixtures with low heat release rates at relevant RCM conditions, such that no pressure waves are generated.

In order for a hot spot to cause mild ignition, two processes must occur. First, the mixture must ignite, releasing stored chemical enthalpy and creating a flame kernel. We define quenching as the phenomenon

Correspondence to: scott.goldsborough@anl.gov

where significant heat release does not occur, and the hot-spot dissipates. Second, this flame kernel must transition into a deflagration wave. Otherwise, the flame kernel extinguishes due to stretch and heat loss. In this work, the two pairs of competing processes (ignition/quenching and flame propagation/extinction) are parametrically investigated using direct numerical simulations.

3 Methodology

Simulations are performed using the ASURF (Adaptive Simulation of Unsteady Reacting Flow) combustion solver, a direct numerical simulation (DNS) code [7,8]. The details of the governing equations, numerical schemes, initial and boundary conditions, and validation can be found elsewhere [7–12]. A reflective boundary condition is used at the wall to simulate a constant volume condition. An initial Gaussian temperature profile is given by equation (1), where T represents temperature, r radius, T_0 the temperature field far from the hot-spot (assumed to be uniform), r_{hot} the characteristic hot-spot radius, and T_{hot} the temperature at the center of the hot-spot. The normalized hot-spot temperature is defined as $T' = T_{hot}/T_0$.

$$T = T_0 \left(1 + \left({}^{T_{hot}}/_{T_0} - 1\right) \exp\left(-\left({}^{r}/_{r_{hot}}\right)^2\right)\right) \quad (1)$$

Simulations are performed in a 2 cm domain with adaptive grid sizes from 3.9 μm to 500 μm. The chemical kinetic model of Kéromnès *et al.* [13] is used in all simulations, where this is one of the most reliable syngas models presently available [14]. Homogeneous ignition and freely propagating flames are calculated using the Cantera software [15]. Results from these simulations, such as homogeneous ignition delay times (τ_{ig}) and unstretched laminar flame speeds (s_L^0), are used throughout this work.

4 Results and Discussion

4.1 Hot-spot quenching and flame ignition

Simulations are first performed for a syngas mixture of 80/20 CO/H_2 at $\phi = 0.5$ in air (Mixture 4 from [16]) at 14.5 atm, 1080 K. Two hot-spot sizes are investigated where we see two behaviors – hot-spot quenching and flame ignition. These are demonstrated in Fig. 1, which presents temperature profiles at early times. The smaller hot-spot (blue, $r_{hot} = 50$ μm) diffusively quenches before ignition can occur, while the larger hot-spot (green, $r_{hot} = 200$ μm) loses heat more slowly, such that ignition occurs followed by flame propagation. Ignition behavior for a range of hot-spot geometries is shown in Fig. 2. Color represents the time for a flame to form, normalized by the homogeneous ignition delay time. Flame formation is defined as the time when the maximum temperature gradient in the domain reaches a value of at least 20% of the maximum temperature gradient in a steady, 1D Cantera flame simulation. A value of 1.0 (yellow) indicates hot-spot quenching with no flame formation, while a value of 0.0 (dark blue) indicates immediate ignition and flame propagation. The black contour at $t/\tau_{ig} = 0.9$ is used in this work to demarcate hot-spot quenching from flame ignition. As expected, flame propagation is more likely with larger values of r_{hot} and T_{hot}.

$$Da_{mix} = \frac{\tau_{heat\ loss}}{\tau_{ig}} \approx \frac{{r_{hot}}^2/\propto}{\tau_{ig,10\%}} \quad (2)$$

For low hot-spot energies expected in engines and rapid compression machines, flame kernel initiation is expected to be governed by the competition between heat loss and ignition time within the hot-spot. This is determined by the scalar mixing Damkohler number, defined in Eq. 2**Fehler! Verweisquelle konnte nicht gefunden werden.**, where α is the thermal diffusivity of the mixture and $\tau_{ig,10\%}$ is the homogeneous ignition delay at a temperature of T_0+0.9(T_{hot} - T_0), as defined

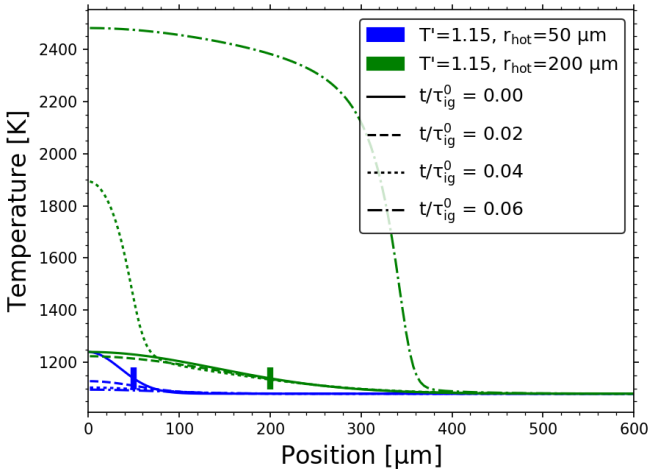

Figure 1: Hot-spot quenching and flame ignition for two different hot-spot geometries (r_{hot} and T_{hot}). Initial hot-spot radius is indicated by the vertical tick mark.

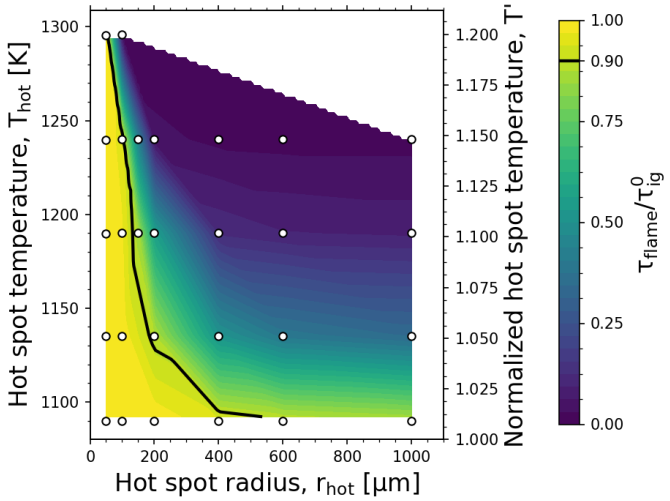

Figure 2: Hot-spot quenching and flame ignition behavior over a range of hot-spot conditions for CO/H_2 = 80/20, ϕ = 0.5 in air, 14.5 atm, T_0 = 1080 K

in [17]. In order to ignite a flame, the ignition delay time at conditions in the hot-spot must be less than the time for the elevated thermal energy of the hot-spot to dissipate, so Da_{mix} >> 1. Figure 3 illustrates fairly

good agreement between Da_{mix} = 7.5 and the boundary between flame ignition and quenching in detailed simulations. This agreement is observed over various values of ϕ and T_0.

4.2 Flame Propagation and Extinction

Fuel transport properties significantly affect the flame propagation processes for large hydrocarbon fuels, especially at lean conditions where the fuel is the deficient reactant. In order to isolate these effects, simulations are performed at ϕ = 0.2 where the fuel transport properties are modified to replicate those of iso-octane (taken from [18]). This modification does not significantly affect the competition between quenching and ignition in detailed simulations (solid lines, black vs. yellow in Fig. 3) and has no visible effect on the mixing Damkohler number (dashed lines). However, flame extinction is observed in some hot-spot geometries for the case with modified transport, as shown in Fig. 4. For this mixture with T' = 1.45 and 1.5, quenching occurs for r_{hot} = 100 μm, extinction occurs with r_{hot} = 150 μm, and steady flame propagation is observed with r_{hot} > 150 μm. This extinction phenomenon appears to be governed by the critical radius [19]. Note that the critical radius in [19] is calculated assuming constant energy deposition rate at r = 0, unlike the transient energy deposition in practical systems. The critical radius calculated from theory for conditions presented here is shown in Table 1, where Le is calculated as in [20], flame thickness is calculated as $\delta = {}^{\alpha}/_{S_l}$ [19], and critical radius is taken from Fig. 10b in [19]. The theoretical critical radius agrees well with the detailed simulations. For the condition with modified transport, the calculated critical radius (280 μm) is close to the critical radius in ASURF (~200 μm) as well as the minimum r_{hot} for propagation found in this work, 150 μm. However, for all other conditions investigated, the critical radius is small enough that heat loss effects dominate through $Da_{mix,}$ and the critical radius cannot be extracted directly from ASURF.

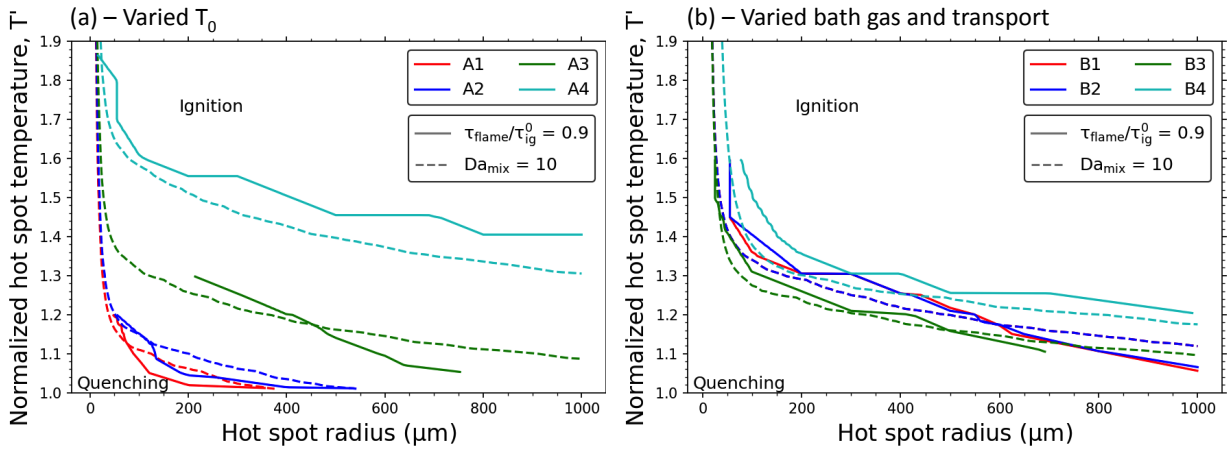

Figure 3: Da_{mix} and boundaries of quenching and ignition covering various hot-spot conditions at different ϕ and T_0. Mixtures are CO/H_2 = 80/20 in air.

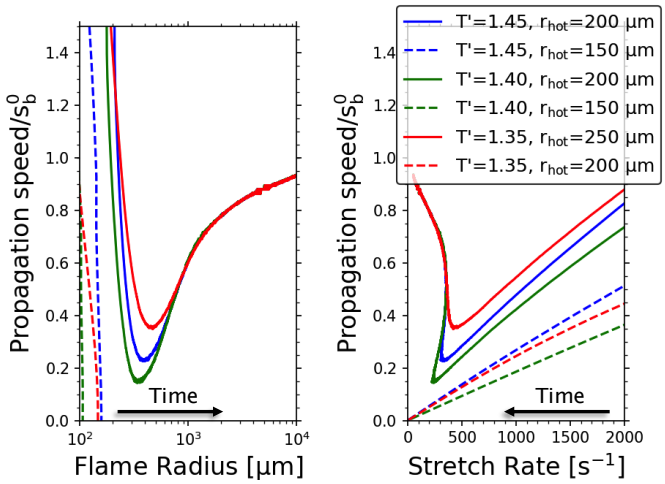

Figure 4: Flame propagation trajectories for various hot-spot conditions at $\phi = 0.2$, $T_0 = 950$ K, P = 14.7 atm. Flame extinction is indicated by propagation speeds rapidly decreasing to zero.

The combined effects of hot-spot quenching and flame extinction are shown schematically in a regime diagram presented in Fig. 5. With low Lewis number, as in the majority of simulations in this work, the critical radius line (blue) only intersects the Damkohler line (orange) at very high hot-spot temperatures. However, under some scenarios, e.g., lean conditions with large hydrocarbon fuels, the critical radius increases, resulting in a flame extinction region that can be observed numerically, and perhaps physically.

Table 1: Theoretical critical radius for present conditions

Condition	Flame thickness (μm)	Le	R_{crit} (μm)
$\phi = 0.5$, 14.7 atm, 1114 K	2.9	0.98	3
$\phi = 0.5$, 14.7 atm, 950 K	3.75	0.99	4
$\phi = 0.2$, 14.7 atm, 950 K	47.7	0.94	36
$\phi = 0.2$, 14.7 atm, 950 K, Modified transport	33.1	1.8	280

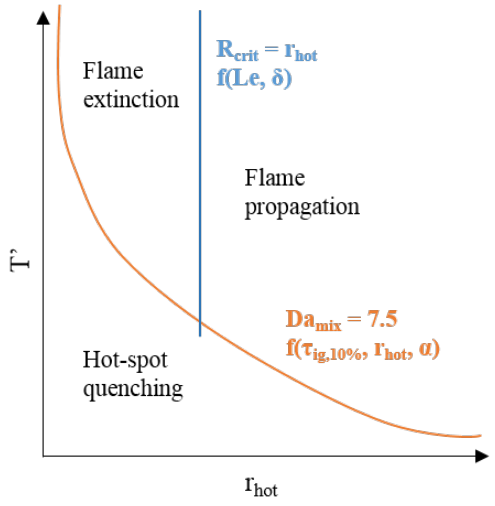

Figure 5: Hot-spot geometry regime diagram

5 Summary

Direct numerical simulations are performed to investigate effects of hot-spot geometry, including size and temperature, on the dynamics of their evolution including quenching, ignition, flame propagation and extinction for syngas mixtures at elevated temperature and pressure. We find that the mixing Damkohler number strongly correlates with the demarcation between quenching and ignition. For very lean conditions with transport properties of iso-octane, a flame extinction region is found, which correlates with a theoretically determined critical radius. From these findings, a regime diagram is created.

Acknowledgements

We thank Weiqi Sun, Zheng Chen, and Yiguang Ju for providing ASURF and helpful discussions. Support is acknowledged through the US DOE Vehicle Technologies Program with Gurpreet Singh and Leo Breton as program managers. Argonne National Laboratory is operated by UChicago Argonne, LLC under Contract No. DE-AC02-06CH11357. The US Government retains for itself, and others acting on its behalf, a paid-up non-exclusive, irrevocable worldwide license in said article to reproduce, prepare derivative works, distribute copies to the public, and perform publicly, by or on behalf of the Government.

References

[1] J.C. Livengood, W.A. Leary, Autoignition by Rapid Compression, Ind. Eng. Chem. 43 (1951) 2797–2805. doi:10.1021/ie50504a046.

[2] C.F. Taylor, E.S. Taylor, J.C. Livengood, W.A. Russell, W.A. Leary, Ignition of Fuels by Rapid Compression, SAE Q. Trans. (1950).

[3] C. Strozzi, A. Mura, J. Sotton, M. Bellenoue, Experimental analysis of propagation regimes during the autoignition of a fully premixed methane–air mixture in the presence of temperature inhomogeneities, Combust. Flame. 159 (2012) 3323–3341. doi:10.1016/j.combustflame.2012.06.011.

[4] C. Strozzi, J. Sotton, A. Mura, M. Bellenoue, Experimental and Numerical Study of the Influence of Temperature Heterogeneities on Self-Ignition Process of Methane-Air Mixtures in a Rapid Compression Machine, Combust. Sci. Technol. 180 (2008) 1829–1857. doi:10.1080/00102200802260656.

[5] S.M. Walton, X. He, B.T. Zigler, M.S. Wooldridge, A. Atreya, An experimental investigation of iso-octane ignition phenomena, Combust. Flame. 150 (2007) 246–262. doi:10.1016/j.combustflame.2006.07.016.

[6] G.T. Kalghatgi, D. Bradley, Pre-ignition and " super-knock " in turbo- charged spark-ignition engines, 13 (2012) 399–414. doi:10.1177/1468087411431890.

[7] Z. Chen, Y. Ju, Studies on the initiation, propagation, and extinction of premixed flames, Princeton University, 2008.

[8] Z. Chen, M.P. Burke, Y. Ju, Effects of Lewis number and ignition energy on the determination of laminar flame speed using propagating spherical flames, Proc. Combust. Inst. 32 (2009) 1253–1260. doi:10.1016/j.proci.2008.05.060.

[9] Z. Chen, M.P. Burke, Y. Ju, On the critical flame radius and minimum ignition energy for spherical flame initiation, Proc. Combust. Inst. 33 (2011) 1219–1226. doi:10.1016/j.proci.2010.05.005.

[10] Z. Chen, On the extraction of laminar flame speed and Markstein length from outwardly propagating spherical flames, Combust. Flame. 158 (2011) 291–300. doi:10.1016/j.combustflame.2010.09.001.

[11] X. Gou, W. Sun, Z. Chen, Y. Ju, A dynamic multi-timescale method for combustion modeling with detailed and reduced chemical kinetic mechanisms, Combust. Flame. 157 (2010) 1111–1121. doi:http://dx.doi.org/10.1016/j.combustflame.2010.02.020.

[12] W. Sun, X. Gou, H.A. El-Asrag, Z. Chen, Y. Ju, Multi-timescale and correlated dynamic adaptive chemistry modeling of ignition and flame propagation using a real jet fuel surrogate model, Combust. Flame. 162 (2015) 1530–1539. doi:10.1016/j.combustflame.2014.11.017.

[13] A. Kéromnès, W.K. Metcalfe, K.A. Heufer, N. Donohoe, A.K. Das, C.-J. Sung, et al., An experimental and

detailed chemical kinetic modeling study of hydrogen and syngas mixture oxidation at elevated pressures, Combust. Flame. 160 (2013) 995–1011. doi:10.1016/j.combustflame.2013.01.001.

[14] C. Olm, I.G. Zsély, T. Varga, H.J. Curran, T. Turányi, Comparison of the performance of several recent syngas combustion mechanisms, Combust. Flame. 162 (2015) 1793–1812. doi:10.1016/j.combustflame.2014.12.001.

[15] D.G. Goodwin, H.K. Moffat, R.L. Speth, Cantera: An object-oriented software toolkit for chemical kinetics, thermodynamics, and transport processes, (2016). http://www.cantera.org.

[16] D.M. Kalitan, J.D. Mertens, M.W. Crofton, E.L. Petersen, Ignition and Oxidation of Lean CO/H2 Fuel Blends in Air, J. Propuls. Power. 23 (2007) 1291–1303. doi:10.2514/1.28123.

[17] P. Pal, A.B. Mansfield, P.G. Arias, M.S. Wooldridge, H.G. Im, A computational study of syngas auto-ignition characteristics at high-pressure and low-temperature conditions with thermal inhomogeneities, Combust. Theory Model. 19 (2015) 587–601. doi:10.1080/13647830.2015.1068373.

[18] M. Mehl, W.J. Pitz, C.K. Westbrook, H.J. Curran, Kinetic Modeling of Gasoline Surrogate Components and Mixtures under Engine Conditions, Proc. Combust. Inst. 33 (2011) 193–200.

[19] Z. Chen, Y. Ju, Theoretical analysis of the evolution from ignition kernel to flame ball and planar flame, Combust. Theory Model. 11 (2007) 427–453. doi:10.1080/13647830600999850.

[20] J.K.K. Bechtold, M. Matalon, The dependence of the Markstein length on Stoichiometry, Combust. Flame. 127 (2001) 1906–1913. doi:10.1016/S0010-2180(01)00297-8.